Liquid Crystals
Publication details, including instructions for authors and subscription information:
http://www.informaworld.com/smpp/title~content=t713926090

Phase equilibrium of poly(*n*-butyl acrylate) and E7

T. Bouchaour; F. Benmouna; L. Leclercq; B. Ewen; X. Coqueret; M. Benmouna; U. Maschke

Online publication date: 06 August 2010

To cite this Article Bouchaour, T. , Benmouna, F. , Leclercq, L. , Ewen, B. , Coqueret, X. , Benmouna, M. and Maschke, U.(2000) 'Phase equilibrium of poly(*n*-butyl acrylate) and E7', Liquid Crystals, 27: 3, 413 — 420
To link to this Article: DOI: 10.1080/026782900202877
URL: http://dx.doi.org/10.1080/026782900202877

LIQUID CRYSTALS, 2000, VOL. 27, NO. 3, 413–420

Phase equilibrium of poly(*n*-butyl acrylate) and E7

T. BOUCHAOUR, F. BENMOUNA, L. LECLERCQ,† B. EWEN,†
X. COQUERET,‡ M. BENMOUNA and U. MASCHKE‡*

University Aboubakr Belkaïd, Institut of Chemistry, Bel Horizon, BP119,
13000 Tlemcen, Algeria
†Max-Planck-Institut für Polymerforschung, Postfach 3148, D-55121 Mainz,
Germany
‡Université des Sciences et Technologies de Lille,
Laboratoire de Chimie Macromoléculaire, Bâtiment C6, CNRS UPRESA N° 8009,
F-59655 Villeneuve d'Ascq Cedex, France

(*Received 17 May 1999; in final form 1 October 1999; accepted 14 October 1999*)

The experimental equilibrium phase diagram of mixtures of linear poly(*n*-butyl acrylate) of molecular mass $M_w = 112\,000$ g mol^{-1} and the low molecular mass LC mixture E7 has been established using polarized optical microscopy and light scattering techniques. The diagram is found to be reminiscent of an upper critical solution temperature system. Two independent series of samples with the same composition were studied, yielding consistent results. A region of nematic and isotropic coexisting phases and a region of a single isotropic phase were identified in the composition–temperature phase diagram. The results were analysed within a theoretical model combining the Flory–Huggins lattice theory for isotropic mixing and the Maier–Saupe theory for nematic ordering. Interestingly, no region of isotropic coexisting phases was observed in our experiments. This is probably due to the fact that the nematic interaction overwhelms the isotropic interaction in the region where (I + I) coexisting phases could appear. A preferential solubility of certain constituents of the LC mixture in the polymer could possibly be a reason for this behaviour.

1. Introduction

Blends of polymers and low molecular mass liquid crystals (LCs) are subjects of fundamental and technological interest [1, 2]. Polymer dispersed liquid crystals (PDLCs), consisting of micron-sized LC droplets dispersed in a polymer matrix, have a considerable potential for a variety of optoelectronic applications [3–6].

The electro-optical properties of polymer/LC blends depend particularly on the size, shape, number density and spatial distribution of the LC droplets. These parameters are generally determined by the kinetics and thermodynamics of the phase separation mechanism, and therefore it is important to understand the phase behaviour of polymer/LC mixtures. In recent years, several studies have been reported along these lines, focusing generally on the determination of the clearing temperature versus composition by polarized optical microscopy (POM), differential scanning calorimetry (DSC) and light scattering (LS) techniques [7–12]. It is beyond the scope of the present paper to give full details of all the results reported in the literature. We will limit ourselves to systems obtained by a solvent-induced phase separation (SIPS) process, followed by a thermally-induced phase separation (TIPS) mechanism. For example, Ahn *et al.* [7] studied the phase behaviour of poly(methyl methacrylate) (PMMA)/7CB and poly(styrene) (PS)/7CB, whereas Carpaneto *et al.* [8] considered the case of poly(*n*-butyl methacrylate)/E7 and PMMA/E7 mixtures. The phase properties of poly(benzyl methacrylate)/E7 [9], PS/E7 [10], PMMA/E7 [11] and functionalized PMMA/E7 [12] were also investigated using the techniques mentioned above.

In this paper, the equilibrium phase diagram of linear poly(*n*-butyl acrylate) and E7 is obtained by POM and LS. Two different aspects of the phase diagram are studied. The variation of the clearing temperature versus composition is obtained together with the formation of the nematic droplets inside the phase diagram. Few experimental results are reported in the literature combining both features. The nematic–isotropic transition temperature was observed using the two techniques indicated earlier. The results are analysed using a theoretical model combining the Flory–Huggins lattice theory for isotropic mixing [13] and the Maier–Saupe theory for nematic ordering [14]. The second problem considered here deals with the development of sample textures

*Author for correspondence, e-mail: maschke@univ-lille1.fr

below the clearing temperature, and hence inside the phase diagram. The changes in shape, distribution and size of the nematic droplets dispersed in the polymer matrix were observed as a function of composition and temperature.

2. Experimental

2.1. *Materials*

Poly(*n*-butyl acrylate) was prepared by a radically-induced polymerization technique using 2,2′-azoisobutyronitrile as initiating species [15]. The poly(*n*-butyl acrylate) was purified and characterized by gel permeation chromatography (GPC) and LS. LS measurements were performed for solutions in toluene at 20°C and $\lambda = 632.8$ nm, yielding $M_w = 112\,000$ g mol^{-1}. The broadness of the molecular weight distribution was measured by GPC in toluene giving $M_w/M_n = 2.2$. The glass transition temperature of the pure polymer was obtained by DSC as $T_g = -55$°C.

The eutectic LC mixture E7 was purchased from Merck Ltd (Poole, GB); it contains 51 wt % of 4-cyano-4′-*n*-pentylbiphenyl (5CB), 25 wt % of 4-cyano-4′-*n*-heptylbiphenyl (7CB), 16 wt % of 4-cyano-4′-*n*-octyloxybiphenyl (8OCB), and 8 wt % of 4-cyano-4″-*n*-pentyl-*p*-terphenyl (5CT). Nevertheless, E7 exhibits a single nematic–isotropic transition temperature $T_{NI} = 60$°C.†

2.2. *Sample preparation*

Sample preparation was made following a combination of SIPS and TIPS. The polymer and E7 were dissolved in a common organic solvent (tetrahydrofuran, THF) at a concentration of 50 wt % at room temperature. The resulting mixture was stirred mechanically overnight. A small quantity of the mixture was cast on a clean glass slide, and the sample was dried at room temperature for two days. After complete evaporation of the THF, another glass slide was put on top of the first one. Samples with pure components have been prepared in a similar way to the polymer/LC blends. The phase behaviour is the same as in the case of samples prepared without the use of THF.

For each composition, the measurements were made on two independent samples. The same results have been found at all compositions within the experimental error.

2.3. *Microscopy*

The thermo-optical studies were performed on a Jenapol POM, equipped with a Linkam THMS 600 heating/cooling stage and a Linkam TMS 92 temperature control unit. All samples were submitted to the same treatment. They were first heated at a rate of 100°C min^{-1} to 70°C and more (depending on the composition) to ensure that a homogeneous isotropic state had been reached. After 5 min, the sample was quenched at a rate of 100°C min^{-1} to a lower temperature selected for observation of the texture. After waiting 5 min, micrographs were taken by means of a video-camera (JVC TK-1070E) and printed on high density paper to record the textures, choosing several regions of the sample (border and centre). It was checked on a few selected samples that waiting longer times, of the order of half an hour, did not lead to different textures. The same procedure was repeated a few times (depending on the composition), with a quench being made from the isotropic state to a temperature different from that of the preceeding quench. At low temperatures, steps of 10°C were selected and in the vicinity of the transition temperature, steps of 1°C were used.

†Value given by Merck Ltd, Merck House, Poole, UK.

2.4. *Light scattering*

Light scattering measurements were performed using the classical set-up illustrated in figure 1 of ref. [16]. The He-Ne Laser ($\lambda = 632.8$ nm) was polarized linearly, perpendicular to the scattering plane. The scattered intensity was measured in the VV mode (I_{vv}), where the analyser axis is parallel to the polarization direction of the incident beam. The scattering pattern was recorded by a CCD camera. No anisotropic effects were found on the intensity pattern, allowing us to perform radial averages of the scattered intensity. The samples already used for POM measurements were submitted to the same heating/cooling cycle as described in the previous section. In the isotropic state at temperatures above 70°C, the scattering intensity was constant and had low values. The temperature at which the scattering intensity underwent a sharp or discontinuous increase was taken as the onset of phase separation.

3. Results and discussion

3.1. *Temperature transition data and theoretical interpretation*

Figure 1 shows the nematic–isotropic transition temperature versus LC composition as obtained by POM and LS. There is good agreement between the two sets of data. Two distinct regions are observed. Below the data points, two phases are in equilibrium, a polymer rich phase in which the LC is isotropic and coexists with a practically pure LC nematic phase. The diagram shows that at a room temperature of 20°C, the solubility limit of E7 in poly(*n*-butyl acrylate) is close to 30%. At higher temperatures, the polymer/E7 mixture gives a single isotropic phase. Interestingly, this diagram does not contain a region of equilibrium between isotropic phases (I + I), probably because the critical temperature

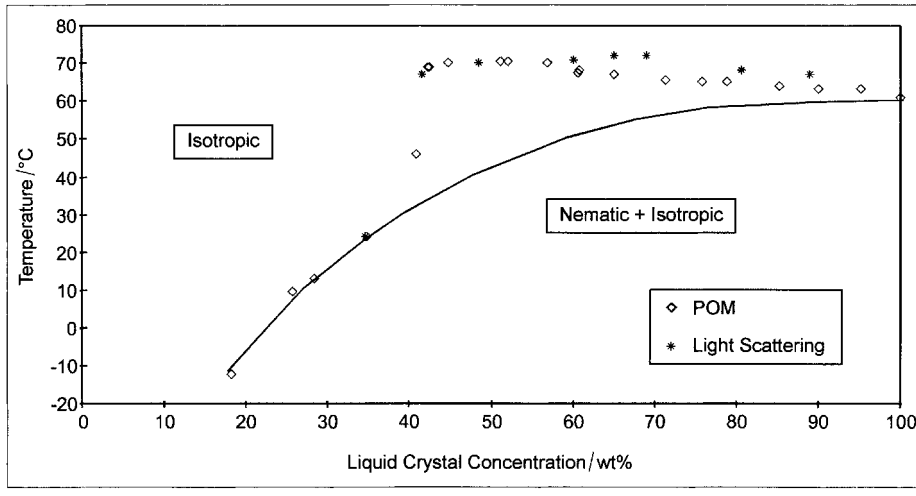

Figure 1. Equilibrium phase diagram of poly(*n*-butyl acrylate) (M_w = 112 000 g mol^{-1})/E7. The symbols in this diagram represent experimental data obtained by POM and LS. At temperatures above the experimental data, an isotropic phase has been found. Below the symbols, a region of coexisting nematic and isotropic phases was detected. The solid curve represents the calculated binodal using the following parameters: $N_1 = 1$, $N_2 = 100$, $\chi = -0.78 + 455/T$.

for isotropic mixing is too low and the nematic interaction overwhelms the isotropic interaction in this region where (I + I) is expected. This reason is likely to be the explanation as to why (I + I) is not observed, since the region of coexisting nematic and isotropic phases (N + I) extends to a temperature range exceeding T_{NI}. E7 is known to be an eutectic mixture of four distinct LC constituents, but is characterized by a single nematic–isotropic transition temperature $T_{NI} = 60°C$. Nevertheless, as a conjecture, we would like to invoke the possibility that these constituents may have different solubilities in the poly(*n*-butyl acrylate) which would lead to a preferential solvation of some of them. This would result in a different composition of the LC in the droplets compared with the E7 mixture. A similar behaviour has already been observed by Nolan *et al.* for ultraviolet cured 40 wt % Norland/60 wt % E7 mixtures [17]. These authors observed a nematic–isotropic transition temperature at $T_{NI} = 65.6°C$. This temperature is significantly higher than the T_{NI} of pure E7 and was interpreted in terms of a loss of miscibility of the higher molecular mass constituents of E7 in the polymer matrix. At this stage, and concerning the phase diagram of the system under investigation here, the preferential solvation of E7 components is only a conjecture which requires more studies to enable one to draw a definite conclusion. Therefore, as long as such a hypothesis is not confirmed, we do not pursue the analysis along these lines and rather use the simple theoretical approach assuming that E7 is characterized by the known $T_{NI} = 60°C$.

A more detailed analysis of the experimental data can be performed with the help of a theoretical framework describing the phase behaviour. In this respect, the solid line of figure 1 represents the calculated binodal curve using a combination of the Flory–Huggins lattice theory for isotropic mixing and the Maier–Saupe theory for the anisotropic ordering [13, 14]. The total free energy in this case is a sum of the isotropic and the nematic free energies indicated by the superscript i and n, respectively.

$$\frac{f^{(i)}}{k_B T} = \frac{F^{(i)}}{n_0 k_B T} = \frac{\varphi_1}{N_1} \ln \varphi_1 + \frac{\varphi_2}{N_2} \ln \varphi_2 + \chi \varphi_1 \varphi_2 \quad (1)$$

$$\frac{f^{(n)}}{k_B T} = \frac{F^{(n)}}{n_0 k_B T} = \frac{\varphi_1}{N_1}\left(- \ln Z + \frac{1}{2} v \varphi_1 S^2 \right) \quad (2)$$

where φ_1 and φ_2 are the volume fractions of LC and polymer, respectively. Assuming incompressibility and equality of molar volumes of species 1 and 2, one has $\varphi_1 = 1 - \varphi_2$. N_1 and N_2 are the numbers of repeat units for molecules of each species; χ is the Flory–Huggins interaction parameter for isotropic mixing. This parameter is assumed to be a function of temperature according to $\chi = A + B/T$, where A and B are constants independent of temperature and composition. The quadrupole interaction parameter v is proportional to the ratio T_{NI}/T with a proportionality factor 4.54. S is the nematic order parameter which is a function of temperature and composition and can be calculated according to the method described in [18–20]. In equation (2), Z represents the anisotropic partition function.

The composition of two coexisting phases α and β can be obtained in general by equating the chemical potentials of the two constituents of the blend in the two phases

$$\mu_1^{(\alpha)} = \mu_1^{(\beta)} \quad (3)$$

$$\mu_2^{(\alpha)} = \mu_2^{(\beta)} \quad (4)$$

where in the present system the chemical potentials are sums of isotropic and nematic contributions

$$\frac{\mu_1}{k_B T} = \ln \varphi_1 + \left(1 - \frac{N_1}{N_2}\right)\varphi_2 + \chi N_1 \varphi_2^2 - \ln Z + \frac{v\varphi_1^2 S^2}{2} \tag{5}$$

$$\frac{\mu_2}{k_B T} = \ln \varphi_2 + \left(1 - \frac{N_2}{N_1}\right)\varphi_1 + \chi N_2 \varphi_1^2 + \frac{N_2}{N_1}\frac{v\varphi_1^2 S^2}{2}. \tag{6}$$

The first three terms in the right hand side of equations (5) and (6) are isotropic contributions, while the rest come from the nematic free energy. In the present system, the resolution is simplified greatly since the phase diagram exhibits a region where an isotropic polymer-rich phase is in equilibrium with an almost pure nematic LC phase. Therefore, the composition of the pure LC phase is known ($\varphi_1 = 1$), while that of the polymer-rich phase is given simply by solving the equation

$$\frac{\mu_1^{(i)}}{k_B T} = \ln \varphi_1 + \left(1 - \frac{N_1}{N_2}\right)\varphi_2 + \chi N_1 \varphi_2^2 = 0. \tag{7}$$

Solving this equation gives the content of LC (φ_1) dissolved in the polymer matrix and the results are used to plot the solid line in figure 1. Clearly the predictions of this theory depend upon the choice of parameters such as N_1, N_2, T_{NI}, and χ. The number of repeat units of LC, N_1, is fixed to 1 while the degree of polymerization of the polymer, N_2, is approximately the same as the ratio of the molecular masses of poly(*n*-butyl acrylate) to E7. This was taken to be $N_2 = 100$. In the absence of further information on the isotropic mixing properties of poly(*n*-butyl acrylate) and E7, we have adjusted the values of A and B for the temperature dependence of the Flory–Huggins interaction parameter χ to obtain the best fit with the data points on the left hand side of the phase diagram; $\chi = -0.78 + 455/T$. The densities of LC and polymer are taken to be approximately equal in the definition of volume fractions. Discrepancies with data points appear in the composition range between 40 and 80 wt % LC. One could try to improve the agreement between theory and experiment by changing A and B, but within this theoretical formalism, and given the fact that E7 is known to have a single $T_{NI} = 60°C$, it is not possible to obtain a nematic phase above 60°C without invoking other arguments such as a compositional change within the E7 mixture itself due to a preferential solvation in the polymer.

3.2. *Morphologies of poly(n-butyl acrylate)/E7 blends*

3.2.1. *Description of sample textures*

Figure 2 shows that the phase diagram over the composition range can be divided into five regions distinguished through the shape, size and distribution of the nematic droplets within the sample. These regions are shown clearly in figure 2 where the dashed lines mark a qualitative change of texture within each region. In figure 2 the (T/composition)-phase diagram has been broken down into regions where characteristic textures are observed. This breakdown is made from a careful observation of the textures under the microscope by changing the temperature following the protocol described earlier for each sample. A large number of microphotographs were taken; the analysis of all textures taken by changing the illuminated region several times for each sample enabled us to produce a characteristic texture for the region under consideration. The schemes given in figures 3(*a*)–3(*m*) represent the typical textures in each region.

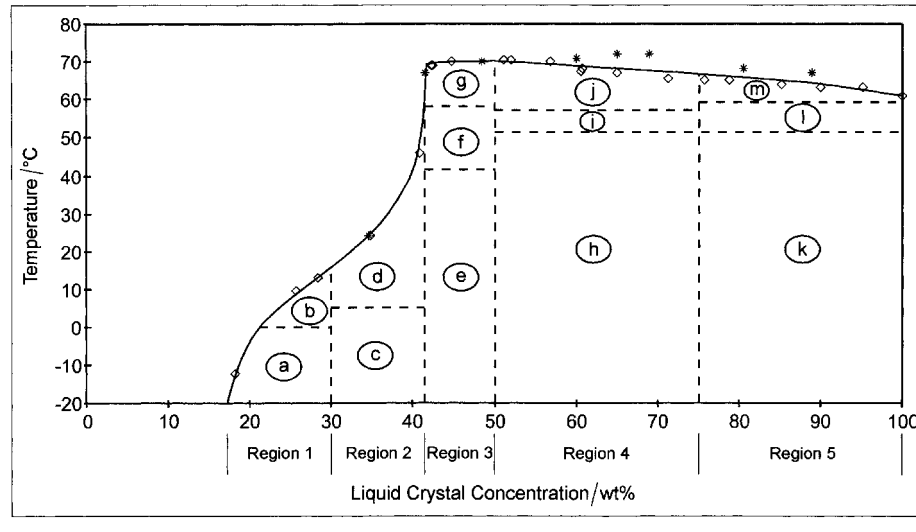

Figure 2. The same experimental data as in figure 1. This diagram has been divided in five regions separating thirteen zones. Dashed lines indicate the divisions between these zones, which are presented in figures 3(*a*)–3(*m*). The continuous line represents a guide line for the eye.

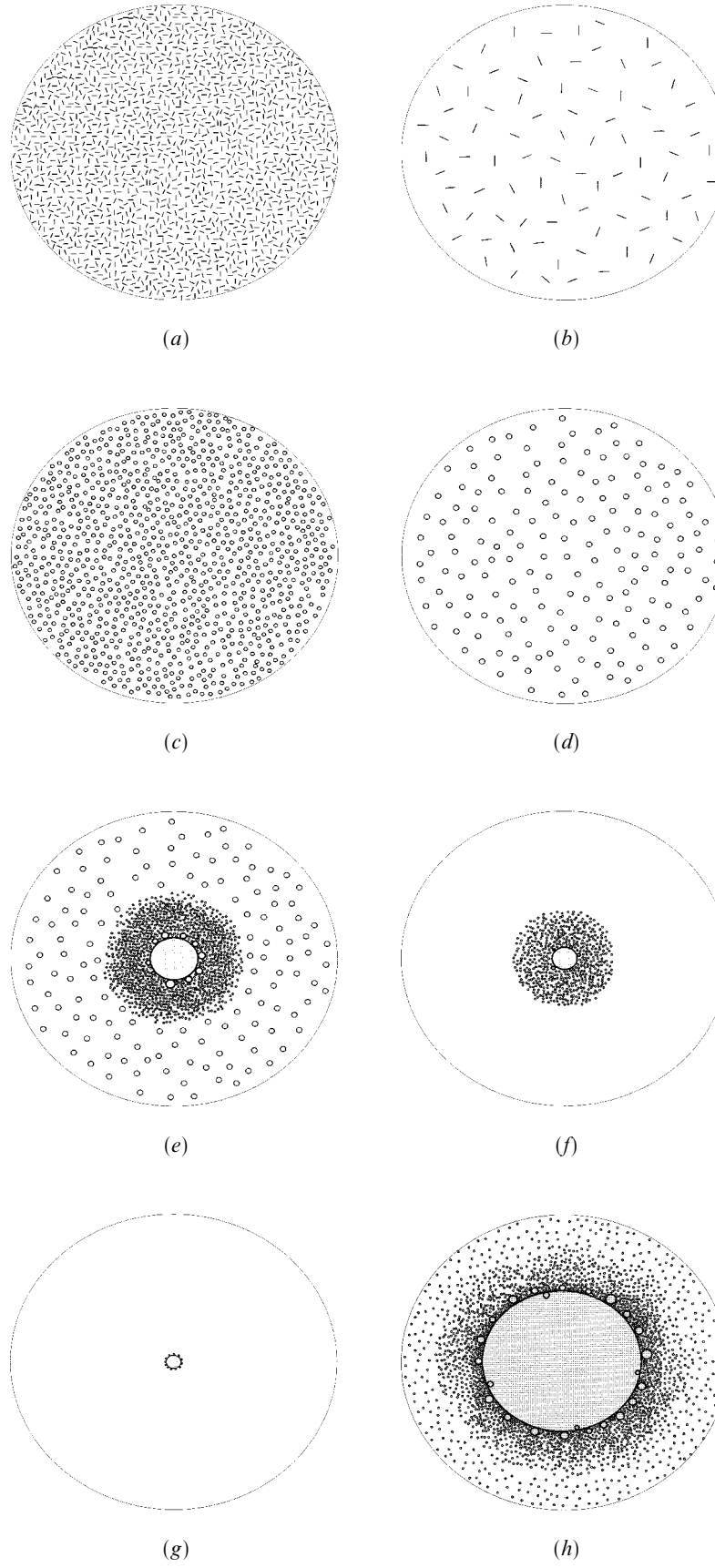

Figure 3. Representative descriptions of the textures revealed by POM corresponding to the regions and zones indicated in figure 2. For example, figure 3 (*a*) corresponds to zone a (region 1) in figure 2 and figure 3 (*h*) corresponds to zone h (region 4). The large spherical droplet in figure 3 (*e*) has an average diameter of 61 μm. This measurement has been used as a standard and the other figures, 3 (*a*)–3 (*d*) and 3 (*f*)–3 (*m*), were constructed accordingly.

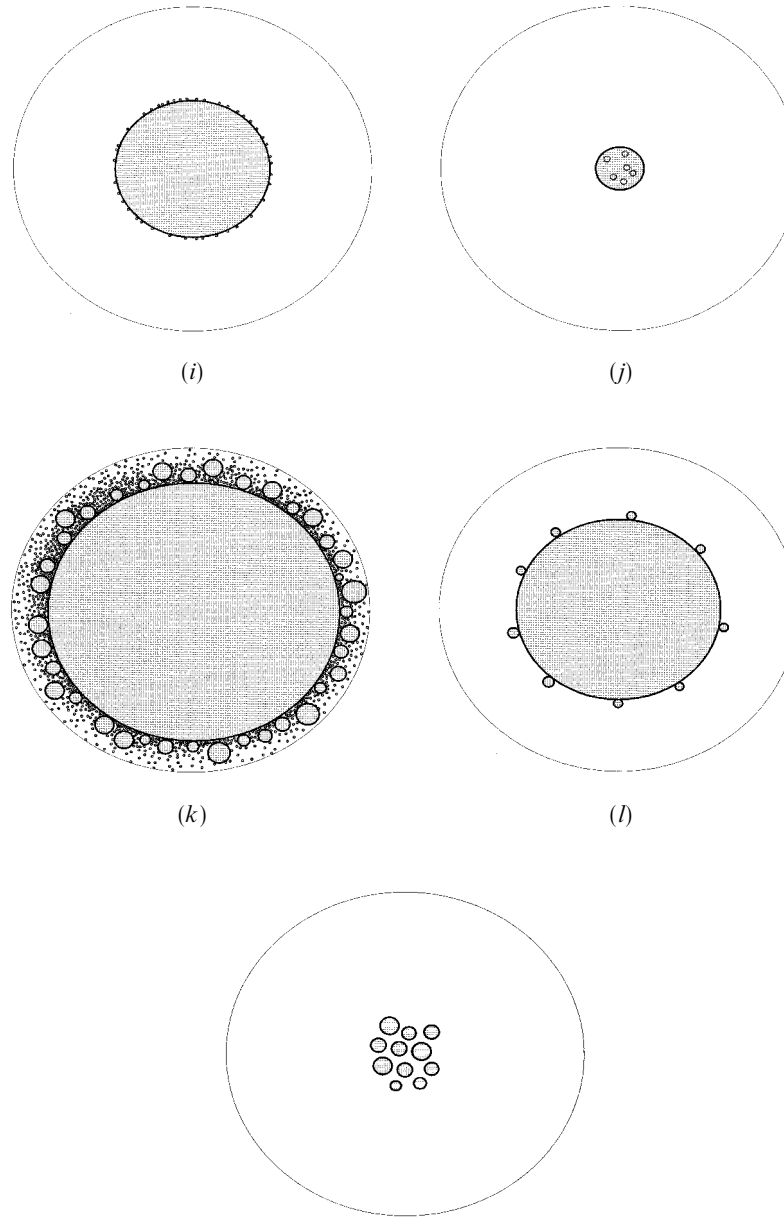

Figure 3. (*continued*).

Region 1 covers the LC composition domain roughly between 15 and 30 wt %. At temperatures below 0°C, the sample shows a dense texture of rod-like droplets distributed homogeneously over the whole sample. A schematic representation of these rod-like droplets is given in figure 3(*a*). Above 0°C, the rods coalesce to form bigger objects with a lower density, coexisting with an isotropic phase which covers a larger area. These coexisting phases are shown on figure 3(*b*). As one crosses the transition temperature, all the droplets disappear and the system exhibits a single isotropic phase.

Region 2 spans the composition range between 30 and 42 wt % LC. The main difference from region 1 is that the droplets have a spherical shape. Their density and size follow similar tendencies seen in the previous case, as illustrated in figures 3(*c*) and 3(*d*).

Region 3 concerns the composition range between 42 and 50 wt % LC. For temperatures below 40°C, a large spherical droplet is formed in the middle of the sample surrounded by small droplets. Above 40°C the size of all droplets decreases, while the isotropic phase forms a corona at the borders of the sample. At the transition

temperature, all the nematic domains melt. Examples of textures illustrating the change of these droplets are shown in figures 3(*e*)–3(*g*).

Similar textures are found between 50 and 75 wt % LC in region 4 except that the radius of the droplet at the centre is much larger and this droplet is surrounded by a thin corona of small droplets. The isotropic phase covers the outer border of the sample. Above 50°C, the droplet at the centre shrinks continuously, while the isotropic region expands more and more. At the clearing temperature, all the small droplets surrounding the central one disappear completely. Figures 3(*h*)–3(*j*) show the development of the droplet size in this region.

Region 5 corresponds to LC compositions above 75 wt %. The droplets remain similar to those of the previous region except that the central droplet is extremely large and covers almost the whole sample. This giant droplet is surrounded by small spheres and isotropic domains. As the temperature increases, the droplet shrinks progressively, while the isotropic phase expands. In the vicinity of the transition temperature, the large droplet breaks into small ones before disappearing completely slightly above 65°C. Examples of textures in this region are given in figures 3(*k*)–3(*m*).

3.2.2. *Variation of the droplet size with composition and solubility limit*

For each composition, the mean diameter of the spherical droplets was determined as a function of temperature. Far below the transition line, this diameter decreases only slightly with temperature. When the transition temperature is approached, a drastic reduction of the droplet size is observed. Figure 4 shows the variation of the mean droplet diameter as a function of composition for two temperatures corresponding to the domain far below the N + I/I transition. The variation of the droplet diameter with the LC concentration is approximately linear at both temperatures. Smith has also observed a similar variation for a poly(urethane)-based polymer/LC system [21]. He pointed out there is no reason for such a behaviour to be general. For example, Golemme *et al.* have found an exponential dependence of the droplet diameter on the LC composition for an epoxy-based system [22].

It has been suggested that the solubility limit can be estimated from the variation of the droplet diameter with composition [21]. A linear fit to the data in figure 4 was performed and extrapolation to the *x*-axis gave results for the solubility limit which are in reasonable agreement with the experimental phase diagram in figure 1.

4. Conclusions

Mixtures of poly(*n*-butyl acrylate) and E7 have been prepared by a combination of SIPS and TIPS processes. An experimental phase diagram of this system obtained by POM and LS techniques exhibited an upper critical solution temperature. The whole phase diagram has been explored in detail revealing different regions. A region with a single isotropic phase and another region

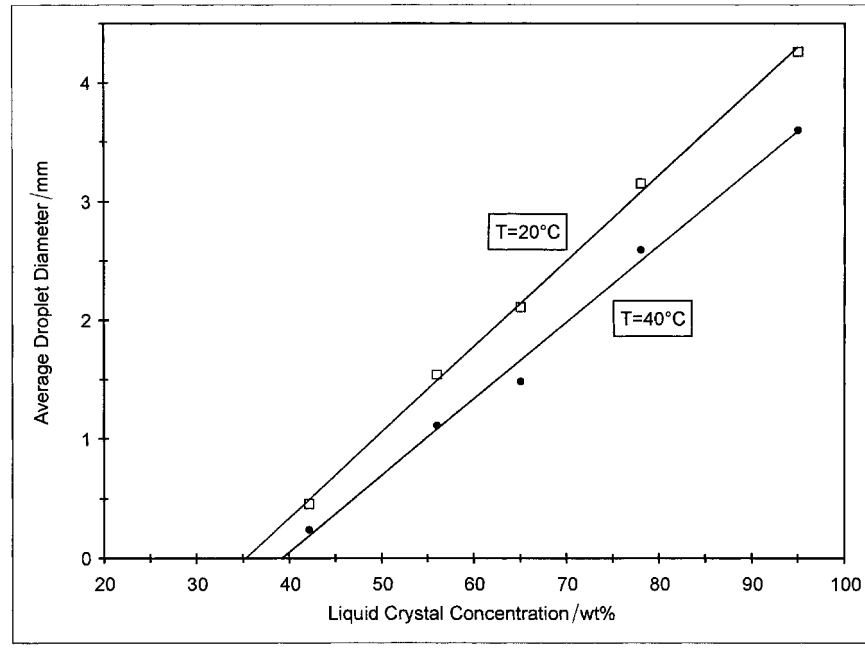

Figure 4. Average droplet diameters evaluated by figures 3(*a*)–3(*m*) as a function of the LC composition for the poly(*n*-butyl acrylate)/E7 system. The symbols □ represent the data for $T = 20$°C, while the symbols ● represent the values for $T = 40$°C. The straight lines represent fits of the experimental data using linear regression analysis. The *x*-axis intercept gives the solubility limit.

where two coexisting (N + I) phases were found in the composition–temperature frame. The LS data agree well with the cloud point curve obtained by POM. A nematic phase coexisting with an isotropic phase was observed even at temperatures higher than T_{NI} of pure E7. This peculiar behaviour could possibly be explained by assuming a preferential solubility of certain constituents of E7 in poly(*n*-butyl acrylate).

The experimental results have been compared with calculations obtained from the Flory–Huggins and the Maier–Saupe theories. Some discrepancies with data in a certain range of LC compositions were found. A conjecture is made to attribute this discrepancy to the preferential affinity of some of the LC constituents for the poly(*n*-butyl acrylate).

The LC solubility limit in the polymer was estimated from the dependence of the mean droplet diameter on the LC concentration and is given by the *x*-axis intercept in figure 4. The results are in good agreement with the experimental cloud point curve.

This work has been accomplished within the scientific agreement CNRS/DRS. The authors thank these organizations for their kind support. L.L. acknowledges the MPG and the CNRS for financial support during his stay at the MPI-P in Mainz. The authors are indebted to Dr M. Bacquet for helpful discussions and to B. Müller of the MPI-P for performing the molecular mass determinations for the polymer.

References

[1] Chandrasekhar, S., 1992, *Liquid Crystals*, 2nd Edn (Cambridge: Cambridge University Press).
[2] De Gennes, P. G., 1974, *The Physics of Liquid Crystals* (London: Oxford University Press).
[3] Doane, J. W., 1990, *Liquid Crystals—Applications and Uses*, Vol. 1, edited by B. Bahadur (Singapore: World Scientific), Chap. 14.
[4] Drzaic, P. S., 1995, *Liquid Crystal Dispersions* (Singapore: World Scientific).
[5] Crawford, G. P., and Zumer, S. (editors), 1996, *Liquid Crystals in Complex Geometries* (London: Taylor & Francis).
[6] (*a*) Maschke, U., Coqueret, X., and Loucheux, C., 1995, *J. appl. polym. Sci.*, **56,** 1547; (*b*) Maschke, U., Gloaguen, J.-M., Turgis, J.-D., and Coqueret, X., 1996, *Mol. Cryst. liq. Cryst.*, **282,** 407; (*c*) Maschke, U., Traisnel, A., Turgis, J.-D., and Coqueret, X., 1997, *Mol. Cryst. liq. Cryst.*, **299,** 371; (*d*) Roussel, F., Buisine, J.-M., Maschke, U., and Coqueret, X.,1997, *Mol. Cryst. liq. Cryst.*, **299,** 321.
[7] Ahn, W., Kim, C. Y., Kim, H., and Kim, S. C., 1992, *Macromolecules*, **25,** 5002.
[8] Carpaneto, L., Ristagno, A., Stagnaro, P., and Valenti, B., 1996, *Mol. Cryst. liq. Cryst.*, **290,** 213.
[9] Shen, C., and Kyu, T., 1995, *J. chem. Phys.*, **102,** 556.
[10] Kim, W.-K., and Kyu, T., 1994, *Mol. Cryst. liq. Cryst.*, **250,** 131.
[11] Kyu, T., Shen, C., and Chiu, H.-W., 1996, *Mol. Cryst. liq. Cryst.*, **287,** 27.
[12] Kyu, T., Ilies, I., Shen, C., and Zhou, Z. L., 1996, in *Liquid Crystalline Polymer Systems—Technological Advances*, edited by A. I. Isayev, T. Kyu and S. Z. D. Cheng (Washington DC: ACS Symposium Series 632), Chap. 13.
[13] Flory, P. J., 1965, *Principles of Polymer Chemistry* (Ithaca: Cornell University Press).
[14] (*a*) Maier, W., and Saupe, A., 1959, *Z. Naturforschung*, **14a,** 882; (*b*) Maier, W., and Saupe, A., 1960, *Z. Naturforschung*, **15a,** 287.
[15] See for example Turgis, J.-D., and Coqueret, X., 1999, *Macromol. Chem. Phys.*, **200,** 652.
[16] Leclercq, L., Maschke, U., Ewen, B., Coqueret, X., Mechernene, L., and Benmouna, M., 1999, *Liq. Cryst.*, **26,** 415.
[17] Nolan, P., Tillin, M., and Coates, D., 1992, *Mol. Cryst. liq. Cryst. Lett.*, **8,** 129.
[18] Brochard, F., Jouffroy, J., and Levinson, P., 1984, *J. Phys. (Paris)*, **45,** 1125.
[19] Shen, C., 1995, PhD thesis, University of Akron, USA.
[20] (*a*) Maschke, U., Coqueret, X., and Benmouna, M., 1997, *Polym. Networks Blends*, **7,** 23; (*b*) Benmouna, F., Bedjaoui, L., Maschke, U., Coqueret, X., and Benmouna, M., 1998, *Macromol. Theory and Simul.*, **7,** 599; (*c*) Benmouna, F., Coqueret, X., Maschke, U., and Benmouna, M., 1998, *Macromolecules*, **31,** 4879; (*d*) Benmouna, F., Maschke, U., Coqueret, X., and Benmouna, M., 1999, *Macromol. Theory and Simul.*, **8,** 479.
[21] Smith, G. W., 1990, *Mol. Cryst. liq. Cryst.*, **180B,** 201.
[22] Golemme, A., Zumer, S., Allender, D. W., and Doane, J. W., 1988, *Phys. Rev. Lett.*, **61,** 2937.